

Experimental study of the $p + {}^6\text{Li} \rightarrow \eta + {}^7\text{Be}$ reaction 11.3 MeV above threshold

A. Budzanowski,¹ A. Chatterjee,² P. Hawranek,³ R. Jahn,⁴ V. Jha,² K. Kilian,⁵ S. Kliczewski,¹ Da. Kirillov,^{5,6} Di. Kirillov,⁷ D. Kolev,⁸ M. Kravcikova,⁹ M. Lesiak,^{3,5} J. Lieb,¹⁰ H. Machner,^{5,6,*} A. Magiera,³ R. Maier,⁵ G. Martinska,¹¹ N. Piskunov,⁷ D. Protić,⁵ J. Ritman,⁵ P. von Rossen,⁵ B. J. Roy,² I. Sitnik,⁷ R. Siudak,¹ R. Tsenov,⁸ J. Urban,¹¹ and G. Vankova^{5,8}

(COSY-GEM Collaboration)

¹*Institute of Nuclear Physics, Polska Akademia Nauk, Radzikowskiego 152, PL-31342 Krakow, Poland*

²*Nuclear Physics Division, Bhabha Atomic Research Centre, Trombay, 400 085-Mumbai, India*

³*Institute of Physics, Jagellonian University, Reymonta 4, PL-30059 Krakow, Poland*

⁴*Helmholtz-Institut für Strahlen- und Kernphysik der Universität Bonn, D-53115 Bonn, Germany*

⁵*Institut für Kernphysik, Forschungszentrum Jülich, D-52425 Jülich, Germany*

⁶*Fachbereich Physik, Universität Duisburg-Essen, D-47048 Duisburg, Germany*

⁷*Laboratory for High Energies, Joint Institute for Nuclear Research, Joliot-Curie 6, 141980 Dubna, Moscow region, Russia*

⁸*Physics Faculty, University of Sofia, 1164 Sofia, Bulgaria*

⁹*Technical University, Kosice, 042 00 Kosice, Slovakia*

¹⁰*Department of Physics, George Mason University, Fairfax, Virginia, USA*

¹¹*P. J. Safarik University, 041 54 Kosice, Slovakia*

(Received 29 June 2010; revised manuscript received 9 September 2010; published 28 October 2010)

The cross section for the reaction $p + {}^6\text{Li} \rightarrow \eta + {}^7\text{Be}$ was measured at an excess energy of 11.28 MeV above threshold by detecting the recoiling ${}^7\text{Be}$ nuclei. A dedicated set of focal plane detectors was built for the magnetic spectrograph Big Karl and was used for identification and four-momentum measurement of ${}^7\text{Be}$. A differential cross section of $\frac{d\sigma}{d\Omega} = [0.69 \pm 0.20(\text{stat.}) \pm 0.20(\text{syst.})]$ nb/sr for the ground state plus $1/2^-$ was measured. The result is compared to model calculations.

DOI: [10.1103/PhysRevC.82.041001](https://doi.org/10.1103/PhysRevC.82.041001)

PACS number(s): 13.75.-n, 25.40.Ve, 25.90.+k

Introduction. The possibility of the η meson to form a quasibound state in a nucleus was first raised by Haider and Liu [1]. Such a state could arise as a consequence of the strongly attractive η -nucleon interaction that is driven by the $N^*(1535)S_{11}$ resonance. By using the s wave ηN scattering length $a_{\eta N} \approx (0.28 + 0.19i)$ fm, Bhalerao and Liu [2] found that the η meson could form a quasibound state with nuclei of mass number $A \geq 10$ [1]. Other groups found similar results when starting from this relatively small value of $a_{\eta N}$ [3,4]. However, Rakityansky *et al.* [5] claimed that an η -nucleus quasibound state may exist for $A \geq 2$, but widths of such quasibound states could be small only for the $\eta^4\text{He}$ system. Binding of the $\eta^4\text{He}$ system was also found in Refs. [6] and [7]. All calculations that span a larger mass scale found that binding increases with increasing mass number.

In a recent study, we found strong evidence that such a quasibound state exists for $\eta \oplus {}^{25}\text{Mg}$ by making use of a two-nucleon transfer reaction $p + {}^{27}\text{Al} \rightarrow {}^3\text{He} + X$ at recoil-free conditions [8] (i.e., the ${}^3\text{He}$ carries the beam momentum, and the bound η is almost at rest). Then, a second step occurs inside the nucleus $\eta + n \rightarrow \pi^- + p$ with the two charged particles being emitted almost back to back. These two charged particles were recorded with a dedicated large acceptance detector [9].

Another approach to search for such quasibound η nuclei is to study the final-state interaction (FSI) in two-body final-state reactions. Recently, two different experiments at the cooler synchrotron at Forschungszentrum Jülich GmbH (COSY) measured η production in $pd \rightarrow \eta^3\text{He}$ reactions very

close to threshold with extremely high-precision data [10,11]. Whereas Smyrski *et al.* [10] claimed that only a scattering length is sufficient to describe the data, Mersmann *et al.* [11] found a better description when an effective range is also taken into account. The result of the first group is $a^3\text{He}\eta = [\pm(2.9 \pm 2.7) + i(3.2 \pm 1.8)]$ fm, while the second group reported $a^3\text{He}\eta = [\pm(10.7 \pm 0.8_{-0.5}^{+0.1}) + i(1.5 \pm 2.6_{-0.9}^{+1.0})]$ fm and $r_0 = [(1.9 \pm 0.1) + i(2.1 \pm 0.2_{-0.0}^{+0.2})]$ fm for the effective range. However, Smyrski *et al.* did not include smearing because of the experimental resolution in the calculation. The nearby pole hypothesis is confirmed by a careful study of the energy dependence of the angular variation [12]. Since the data are not sensitive to the sign of the real part of the scattering length, the quest for a bound state or an unbound pole cannot be answered. The pole position or binding energy is

$$|Q^3\text{He}\eta| \approx 0.30 \text{ MeV}. \quad (1)$$

From the model calculations, it is known that binding is more probable for heavier nuclei than for lighter nuclei. Indeed, in a recent study of the s wave in the $dd \rightarrow \eta\alpha$ reaction [13], which employed a tensor-polarized deuteron beam, a scattering length $a^4\text{He}\eta = [\pm(3.1 \pm 0.5) + i(0 \pm 0.5)]$ fm was found by yielding a pole position,

$$|Q^4\text{He}\eta| \approx 4 \text{ MeV}. \quad (2)$$

Hence, one can expect the binding of η mesons with $A = 7$ nuclei to be even stronger.

Experiment. In this Rapid Communication, we present results of a measurement of η production on ${}^6\text{Li}$:

$$p + {}^6\text{Li} \rightarrow \eta + {}^7\text{Be}. \quad (3)$$

*h.machner@fz-juelich.de

Such a measurement was performed earlier at SATURNE [14] at a proton beam energy of 683 MeV, which corresponds to a momentum of 1322 MeV/c or to an excess energy of 19.13 MeV. Two photons were measured with a two-arm spectrometer. In total, eight events were detected with three, which are believed to stem from background. A differential cross section of $d\sigma/d\Omega = (4.6 \pm 3.8)$ nb/sr was reported. This value corresponds to the sum of the ground and all excited states of ${}^7\text{Be}$ up to about ≈ 10 -MeV excitation. These are the particle-bound states with $L = 1:3/2$ (g.s.) and $1/2$ (0.43 MeV), and particle-unbound states with $L = 3:7/2$ (4.57 MeV) and $5/2$ (≈ 7 MeV) [15]. The reaction was theoretically studied by assuming a reaction $pd \rightarrow \eta^3\text{He}$ with an additional α particle as a spectator [16]. By including the excited states, the experimental cross section could be reproduced. However, the coincidence in values was assumed to be largely fortuitous in view of the large error bars in both the experiment and the prediction.

Here, we report on an experiment, which was conducted even closer to threshold. In contrast to the previous experiment [14], we measured the ${}^7\text{Be}$ nucleus. This reduces the number of possible excited states to only one, since all other excited states are particle unbound. In the next paragraph, we will present the experiment. Then, we will discuss the result and finally state our conclusions.

The experiment was performed at the cooler synchrotron COSY at Jülich. A proton beam of 1310-MeV/c momentum, which corresponds to a beam energy of 673.1 MeV was used. The excess energy for reaction (3) is 11.28 MeV. The recoiling ${}^7\text{Be}$ nuclei were detected with the magnetic spectrograph Big Karl [17,18]. The layout is schematically shown in Fig. 1. Since the rather low-energy Be nuclei are strongly ionizing, a different setup than the usual one in the focal plane had to be developed. All detectors were placed in a box made of steel. Vacuum pumps were mounted on the top. It was flanged with its front side to the exit window of the spectrometer. The window has dimensions 65.5×6.5 cm². On both sides, there are three flanges, which were used to feed the detector

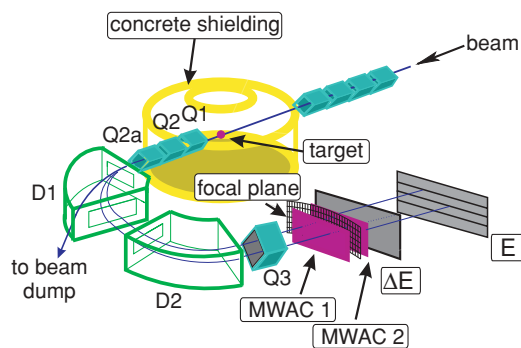


FIG. 1. (Color online) Schematic of the Big Karl setup. The beam is focused with the help of four quadrupole magnets in the beam line onto the target. Quadrupole magnets in the spectrometer are designated as $Q1$, $Q2$, $Q2a$, and $Q3$, whereas $D1$ and $D2$ denote dipole magnets. Multiwire avalanche chambers are denoted by MWACs. ΔE and E are five scintillators, which measure energy and time of flight (TOF). The focal plane detectors are mounted in a vacuum box, which is connected to the vacuum in the magnets.

signals out of the vacuum. Detectors used to measure the reaction-product position, and their emission direction was two multiwire avalanche chambers (MWACs), each of size 70×8 cm². Each chamber had 546 wires inclined by 45° to the left and a similar number inclined to the right. Therefore, they were position sensitive in the horizontal as well as in the vertical directions. Each wire had a diameter of $20 \mu\text{m}$ so that only 0.04% of the chamber area was filled with wire material. The chambers were subdivided into a right and a left half with a separate delay line readout. The response of the chambers to ions was tested with beams of ${}^7\text{Li}$ at 48 MeV, ${}^{12}\text{C}$ at 60 MeV, and ${}^{16}\text{O}$ at 50 MeV delivered from the BARC-TIFR pelletron accelerator at Mumbai.

The two MWACs were followed by two layers of plastic scintillators. The first one was a bar with dimensions 60×8 cm². It had a thickness of 0.5 mm and served as a ΔE detector as well as a start detector for a TOF measurement. The second layer was a stack of four scintillators of 70×2 cm², each 2-mm thick. It served as an E detector as well as a stop detector for the TOF measurement. The distance between ΔE and E detectors was 1.02 m, and that between the two MWACs was 0.445 m.

The incident-beam intensity was measured by calibrated luminosity monitors left and right of the target at large angles. The total number of incident protons was $(6.97 \pm 0.70) \times 10^{13}$. The target was a metallic self-supporting foil produced by rolling to a thickness of $100 \mu\text{m}$. It was isotopically pure to 99%. Its thickness was a compromise between count rate and energy resolution. It was optimized to $100 \mu\text{m}$, which corresponds to an energy resolution of 1 MeV. Hence, it was not possible to separate and to distinguish between the ground state and the first excited state of ${}^7\text{Be}$.

Results. The number of ${}^7\text{Be}$ nuclei is expected to be small so that particle identification is important to distinguish between frequent background and rare events. Therefore, particle identification was performed by redundant methods.

In Fig. 2, the TOF is shown as a function of the momenta of the particles. The ${}^7\text{Be}$ ions were expected to fall between the bands of deuterons plus α particles and ${}^3\text{He}$. Figure 3 shows the relation between TOF and energy of the particles. Also, on this plot, ${}^7\text{Be}$ nuclei can be well separated from other species. Similar selections were performed for $\Delta E - E$ measurements. The loci for different particles were consistent with Monte Carlo simulations.

The obtained missing-mass distribution is shown in Fig. 4. Finally, simulations were performed for multipion production similar to Ref. [13]. The four-pion production has no acceptance in the present setup. Two- and three-pion productions have almost the same missing-mass distribution. We then fitted the distribution to the data except to those in the peak area. This physical background was then subtracted, and the remaining count rate was converted back to integer numbers. This does not introduce a large error, since the background is almost 2.0 in the peak region. For the events that survive all these cuts and after subtracting background, we obtain the missing-mass distribution, which is shown in Fig. 4. A peaklike structure remains, which contains 15 counts. By fitting the pion background simultaneously with a Gaussian yields 12.7 ± 5.0 counts. Therefore, we assume

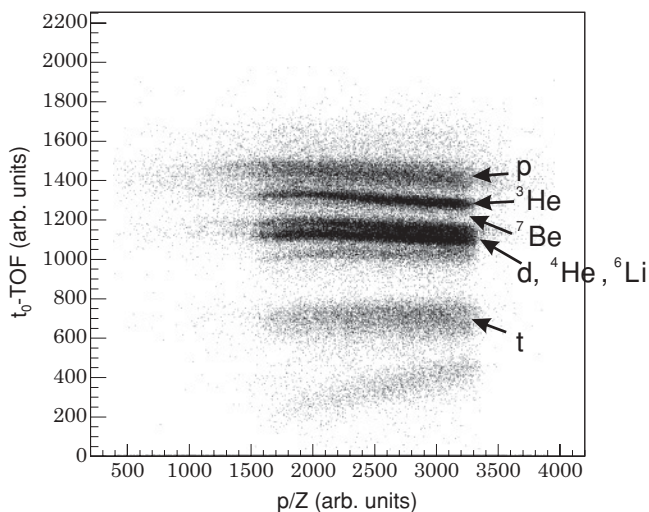


FIG. 2. The time difference due to TOF and the momentum of the particles as measured in MWAC 2.

a systematic uncertainty in the total number of counts of 25%. The number of counts can now be converted into a cross section. For these events, an angular distribution in the c.m. system was deduced, which is shown in Fig. 5. Since we have a small number of counts, we make use of Poisson statistics, which yield asymmetric statistical errors. Systematic uncertainties stem from target thickness (10%), total beam flux (10%), and multipion background (25%). All other uncertainties are much smaller. For the differential cross section, by adding all these uncertainties in quadrature gives a value,

$$\frac{d\sigma}{d\Omega} = [0.69 \pm 0.20(\text{stat.}) \pm 0.20(\text{syst.})] \text{ nb/sr.} \quad (4)$$

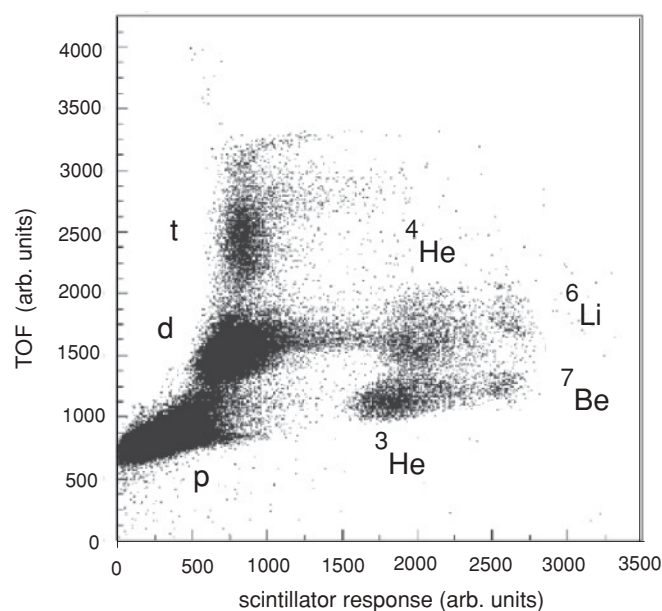


FIG. 3. Scatter plot of TOF as a function of the output of the E scintillator.

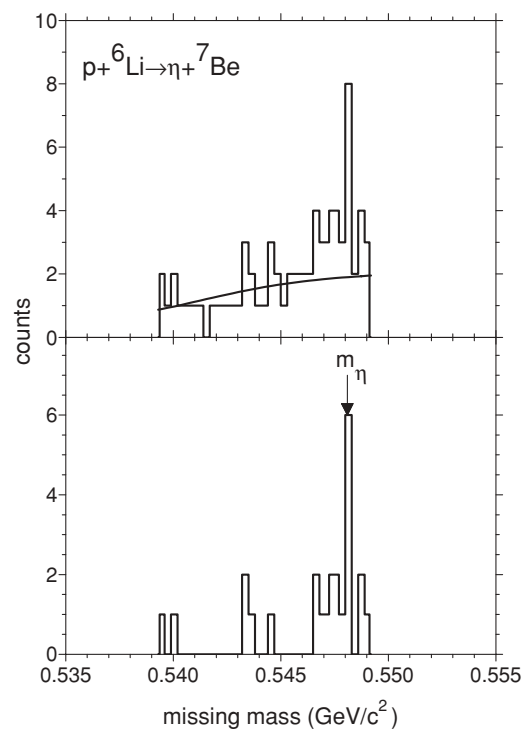


FIG. 4. Upper panel: missing-mass distribution of the $p + {}^6\text{Li} \rightarrow {}^7\text{Be} + X$ reaction. The solid curve is the three-pion production adjusted to the present data, which neglect the peak structure. Lower panel: missing-mass distribution (converted to integer numbers) of the $p + {}^6\text{Li} \rightarrow \eta + {}^7\text{Be}$ reaction after pion background subtraction.

Discussion. This cross section, with two possible final states at an excess energy of 11.28 MeV, is smaller than the number 4.6 ± 3.8 nb/sr quoted for an excess energy of 19.13 MeV and four final states [14]. To make a comparison of the cross sections more meaningful, we subtract the contributions of the $L = 3$ states from the latter experimental result. Al-Khalili *et al.* [16] derived an expression for the differential cross

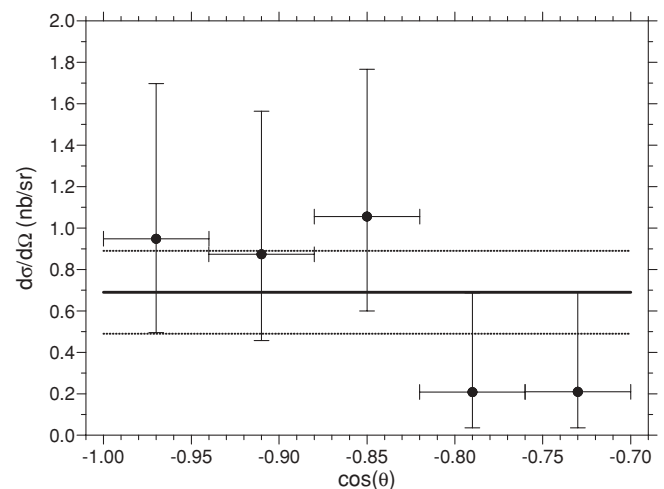


FIG. 5. Angular distribution of the present measurement. The lines show the mean value together with its uncertainty.

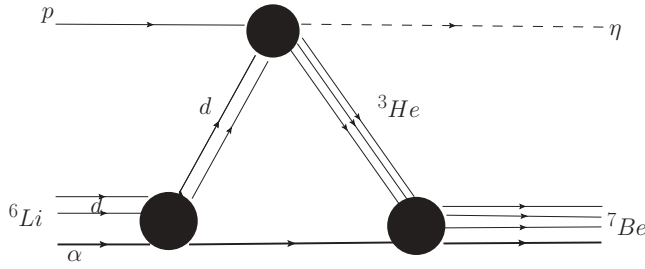


FIG. 6. η -production graph, which treats the α particle (thick line) as a spectator.

section,

$$\frac{d\sigma(p^6\text{Li} \rightarrow \eta^7\text{Be})}{d\Omega} = \mathcal{C} \frac{p_\eta^*}{p_p^*} |f(pd \rightarrow \eta^3\text{He})|^2 \sum_j \frac{2j+1}{2} \mathcal{F}_j^2, \quad (5)$$

with j as the total angular momentum of the final states in ${}^7\text{Be}$ and \mathcal{F}_j as their form factors. \mathcal{C} is the overlap of cluster-wave functions, p_η^* and p_p^* are the c.m. momenta of the final and initial systems, and $|f|$ is the spin-averaged matrix element of the underlying more elementary reaction, which treats the α particle as a spectator. This reaction is illustrated in Fig. 6. We then obtain from Eq. (5),

$$\frac{d\sigma(L=1)}{d\Omega} = \frac{d\sigma(\text{exp.})}{d\Omega} \frac{\sum_{j=3/2,1/2} \frac{2j+1}{2} \mathcal{F}_j^2}{\sum_{j=3/2,1/2,7/2,5/2} \frac{2j+1}{2} \mathcal{F}_j^2}, \quad (6)$$

where the experimental cross section contains contributions from $L=1$ and $L=3$. The resulting value is compared with the present result in Fig. 8. The difference between the two experimental results is now much smaller as expected.

Since new data for the underlying $pd \rightarrow \eta^3\text{He}$ reaction have recently been reported, we have used all data in the vicinity of the threshold [10,11,19,20] to derive $|f|^2 = p_p^*/p_\eta^* \sigma(pd \rightarrow \eta^3\text{He})/d\Omega$ with $p_{p,\eta}^*$ as the c.m. momenta of the initial and final states.

The matrix element $|f|^2$ at 19.13 MeV is now significantly smaller than the value assumed in Ref. [16]. Since the interval of transferred momentum is narrow, we ignore its dependence on the overlap integral and on the form factor and calculate the cross section for the present reaction according to Eq. (5). It is also shown in Fig. 8 as a dashed curve. It accounts for the present measurement and meets the error bar of the earlier measurement. It should be mentioned that the calculation is expected to be correct within 66% because of an uncertainty in $\mathcal{F}_{3/2}^2$. The shape of the resulting curve is almost the same as the one for the $pd \rightarrow \eta^3\text{He}$ reaction. This is so, since the phase factors p_p^*/p_η^* for the underlying reaction and the present reaction are almost identical (see Fig. 7). Therefore, this model cannot give a decisive answer whether a possible pole in FSI moves to a larger Q value for the present reaction.

A more recent calculation was reported by the Mumbai group [21]. Again, the target and the residual nuclei were treated as being composed of two clusters. The input is the η -nucleon interaction where they have assumed a large

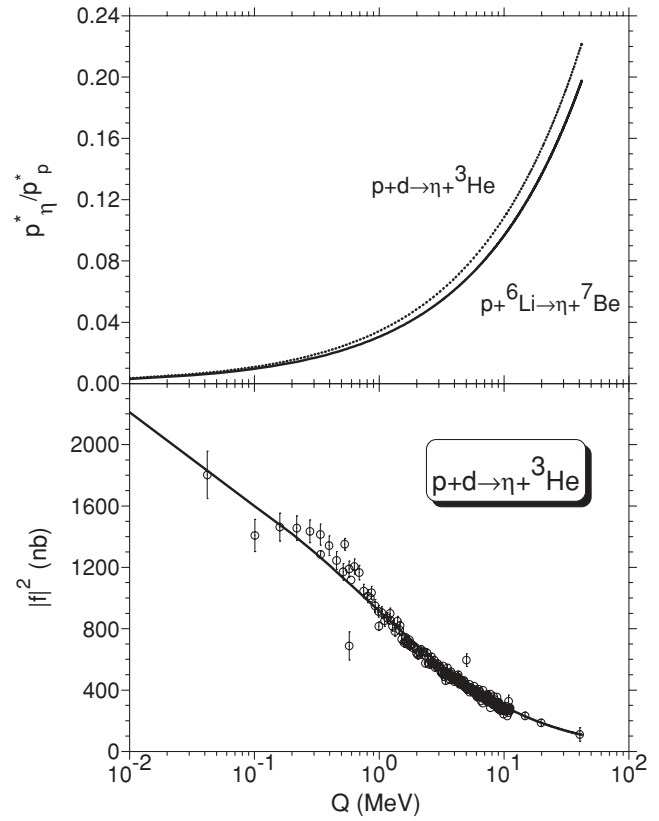


FIG. 7. The energy-dependent quantities that enter the model of Al-Khalili *et al.* [16]. Upper part: the phase-space factor p_η^*/p_p^* for the two indicated reactions. Lower part: the spin-averaged matrix element $|f|^2 = p_p^*/p_\eta^* \sigma(pd \rightarrow \eta^3\text{He})/d\Omega$ as obtained from the data [10,11,19,20]. The solid curve is a fit to the matrix elements.

scattering length in agreement with a bound state. In addition to the graph shown in Fig. 6, they included a rescattering term. Thus, the shape of the excitation function becomes different than the one for the underlying $pd \rightarrow \eta^3\text{He}$ reaction. Their results where the cluster-wave functions were generated by the Woods-Saxon potential are also shown in Fig. 8. Here, we have divided their result for the total cross section by 4π . This calculation with a rather large η -nucleon scattering length differs largely from the one within the model of Ref. [16]. The calculation without FSI, which is phase-space behavior, shows the energy dependence of the data but underestimates the measured data. A small FSI cannot be ruled out.

To summarize, we have measured the momentum \vec{p} of ${}^7\text{Be}$ nuclei from the reaction $p + {}^6\text{Li} \rightarrow \eta + {}^7\text{Be}$ at a beam momentum of 1310 MeV/c with the high-resolution magnetic spectrograph Big Karl. Dedicated focal plane detectors were developed and were used: MWACs and $\Delta E - E$ scintillators. The latter permitted TOF measurements. All detectors were working in vacuum. A differential cross section of 0.69 nb/sr in the c.m. system was obtained, which corresponds to a total cross section of $(8.6 \pm 2.6 \text{ stat.} \pm 2.4 \text{ syst.})$ nb when isotropic emission is assumed. This cross section, at an excess energy of 11.28 MeV, is almost an order of magnitude smaller than the number 4.6 ± 3.8 nb/sr quoted for an excess energy

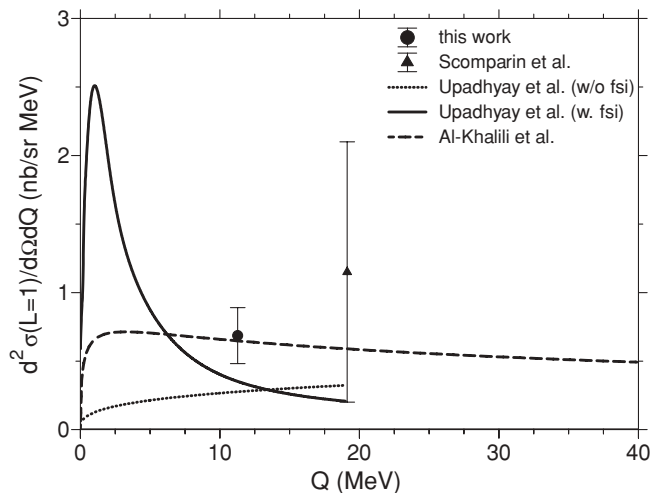


FIG. 8. Excitation function of the reaction $p + {}^6\text{Li} \rightarrow \eta + {}^7\text{Be}$ with Be in its ground state and first excited state. The data are the present measurement (full dot) and, for these states, the corrected result from Ref. [14] (triangle). The calculations based on the model of Ref. [16] are shown as a dashed curve. Those calculations performed in Ref. [21], for the total cross section, were divided by 4π . The calculation with a strong FSI is shown as a solid curve, while the one without FSI is shown as a dotted curve.

of 19.13 MeV [14]. However, in the present experiment, only two possible final states exist, which correspond to angular momentum states with only $L = 1$, while in the earlier experiment, four final states with $L = 1$ and $L = 3$ contribute. Comparison for only $L = 1$ states reduces the difference. The data were compared with model calculations. Although the calculations predict the right order of magnitude, one cannot distinguish the size of the FSI. More data, especially closer to threshold, are necessary to pin down the open problems.

The reactions of η production on light nuclei with two-body final states as discussed earlier and in this Rapid Communication have been performed at energies below the η -production threshold of proton-proton interactions. Different scenarios have been applied to account for such processes, such as multistep processes, interaction of the projectile with a nucleon, which has large Fermi momentum, and coherent interaction. Thus, subthreshold η production on light nuclei is interesting in itself. In addition, η production differs from π^0 production because of its coupling to a resonance [the $N^*(1535)$]. We compare the present total cross section with those for other light nuclei reactions for about the same excess energy. The values are 407 ± 20 nb for the $p + d \rightarrow \eta + {}^3\text{He}$ reaction [11], 16 ± 1.6 nb for the $d + d \rightarrow \eta + {}^4\text{He}$ reaction [13], and for the present $p + {}^6\text{Li} \rightarrow \eta + {}^7\text{Be}$ reaction: $(8.6 \pm 2.6 \text{ stat.} \pm 2.4 \text{ syst.})$ nb. This shows a dramatic decrease in the cross section with an increase in the mass number for the proton-induced reactions. The c.m. momenta in all three reactions are compatible. This is in strong contrast to inclusive production in heavy-ion collisions where a dependence $\sigma \propto (A_p A_t)^{2/3}$ was found [22]. So, the origin of the decrease will be the A dependence of the corresponding form factors at the large momentum transfer of 800–900 MeV/c. This reflects the fact that it is more unlikely to fuse to a heavy system than to a light system.

We are grateful to the COSY crew for preparing an excellent beam. One of us (H.M.) thanks C. Wilkin for fruitful discussions. We appreciate the support received from the European community research infrastructure activity under the FP6 Structuring the European Research Area programme, Contract No. RII3-CT-2004-506078, from the Indo-German bilateral agreement, from the Bundesministerium für Bildung und Forschung, BMBF (Grant No. 06BN108I), from the Research Centre Jülich (FFE), and from GAS Slovakia (Grant No. 1/4010/07).

- [1] Q. Haider and L. C. Liu, *Phys. Lett. B* **172**, 257 (1986).
 [2] R. S. Bhalerao and L. C. Liu, *Phys. Rev. Lett.* **54**, 865 (1985).
 [3] R. Hayano, S. Hirenzaki, and A. Gillitzer, *Eur. Phys. J. A* **6**, 99 (1999).
 [4] C. Garcia-Recio, T. Inoue, J. Nieves, and E. Oset, *Phys. Lett. B* **550**, 47 (2002).
 [5] S. A. Rakityansky, S. A. Sofianos, M. Braun, V. B. Belyaev, and W. Sandhas, *Phys. Rev. C* **53**, R2043 (1996).
 [6] S. Wycech, A. M. Green, and J. A. Niskanen, *Phys. Rev. C* **52**, 544 (1995).
 [7] N. N. Scoccola and D. O. Riska, *Phys. Lett. B* **444**, 21 (1998).
 [8] A. Budzanowski *et al.* (COSY-GEM Collaboration), *Phys. Rev. C* **79**, 061001(R) (2009).
 [9] M. G. Betigeri *et al.*, *Nucl. Instrum. Methods Phys. Res., Sect. A* **578**, 198 (2007).
 [10] J. Smyrski *et al.*, *Phys. Lett. B* **649**, 258 (2007).
 [11] T. Mersmann *et al.*, *Phys. Rev. Lett.* **98**, 242301 (2007).
 [12] C. Wilkin *et al.*, *Phys. Lett. B* **654**, 92 (2007).
 [13] A. Budzanowski *et al.* (The GEM Collaboration), *Nucl. Phys. A* **821**, 193 (2009).
 [14] E. Scomparin *et al.*, *J. Phys. G* **19**, L51 (1993).
 [15] D. Tilley *et al.*, *Nucl. Phys. A* **708**, 3 (2002).
 [16] J. S. Al-Khalili, M. B. Barbaro, and C. Wilkin, *J. Phys. G* **19**, 403 (1993).
 [17] M. Drochner *et al.*, *Nucl. Phys. A* **643**, 55 (1998).
 [18] H. Bojowald *et al.*, *Nucl. Instrum. Methods Phys. Res., Sect. A* **487**, 314 (2002).
 [19] B. Mayer *et al.*, *Nucl. Phys. A* **437**, 630 (1985).
 [20] H. H. Adam *et al.*, *Phys. Rev. C* **75**, 014004 (2007).
 [21] N. J. Upadhyay, N. G. Kelkar, and B. K. Jain, *Nucl. Phys. A* **824**, 70 (2009).
 [22] H. Noll *et al.*, *Phys. Rev. Lett.* **52**, 1284 (1984).